ANAS Transactions Earth Sciences 2 / 2024

http://www.journalesgia.com

PETROGRAPHY AND GEOCHEMISTRY OF THE LOWER CRETACEOUS DEPOSITS OF THE VANDAM ZONE (SOUTHERN SLOPE OF THE GREATER CAUCASUS): INSIGHTS INTO PALEOWEATHERING, PROVENANCE AND TECTONIC SETTING

Guliyev E.Kh.

Ministry of Science and Education of the Republic of Azerbaijan,
Institute of Geology and Geophysics, Azerbaijan
H.Javid Ave., 119, Baku, AZ1143: guliyevemin@outlook.com

Keywords: *provenance, tectonic setting, paleoweathering, Vandam zone, Kepuch and Gyrkhbulag Formations*

Summary. This study examines the paleoweathering conditions, provenance, and tectonic setting of Neocomian deposits, focusing on the Kepuch and Gyrkhbulag Formations within the Vandam tectonic zone on the northern flank of the South-Caucasian microplate, characterized by complex Cretaceous flysch and volcanogenic formations. By integrating petrographic and geochemical data, this research aims to identify distinctive geochemical features reflecting provenance, weathering processes, and depositional environments, deepening the understanding of the regional geodynamic evolution. Petrographic analysis of the sandstones reveals a composition primarily consisting of rock fragments, quartz, and feldspar, with a significant clay matrix exceeding 15%, classifying them as lithic wackes and highlighting the dominance of volcanic and metamorphic rock fragments along with authigenic calcite cement. All geochemical proxies for paleoweathering, such as the Chemical Index of Alteration (CIA), Chemical Index of Weathering (CIW), and Plagioclase Index of Alteration (PIA), suggest that the source regions underwent a low to moderate degree of weathering. Provenance analysis suggests that the sediments are derived from a mixed source, primarily consisting of felsic and intermediate igneous rocks, consistent with a continental island arc tectonic environment. Discrimination diagrams – including SiO_2 versus K_2O/Na_2O, Al_2O_3/SiO_2 versus Fe_2O_3+MgO, La–Th–Sc, Ti/Zr versus La/Sc, and Eu/Eu*–Gd_N/Yb_N – place the samples within active continental margin and continental island arc fields, supporting a subduction-related sediment source. This analysis highlights the significant role of tectonic processes in shaping the geochemical characteristics of these siliciclastic rocks.

Introduction

The geochemistry of sedimentary rocks plays a crucial role in deciphering their provenance, tectonic setting, and the processes involved in their formation. The chemical composition of these rocks is greatly influenced by the nature of their source areas, extent of weathering, and the tectonic environment from which they originate. These multiple factors create distinct geochemical signatures that provide insights into the provenance, depositional conditions, and the tectonic settings. Thus, the application of geochemical techniques, including the analysis of major, trace, and rare earth elements (REE), has become crucial for understanding the tectonic settings of sedimentary rocks, as it sheds light on their provenance, weathering processes, and associated depositional environments (Bhatia, 1983, Bhatia, Crook, 1986; Roser and Korsch, 1986; McLennan, 1993; Floyd & Leveridge 1987; Roeser and Korsch, 1988; Floyd et al. 1990; Schieber, 1992; Rodrigo et. al., 2020; Masidul et.al., 2020; Haunhar et.al., 2021). Moreover, the integration of petrographic and geochemical data has been proved to be a powerful tool to evaluate tectonic setting of deposit.

The Cretaceous deposits on the southern slope of the Greater Caucasus have a well-established history of their study; however, there is a limited amount of research specifically focusing on the petrography and geochemistry of these deposits. This research is dedicated to a comprehensive mineralogical-geochemical analysis of sedimentary facies, aimed at identifying indicative associations within the sedimentary rocks to elucidate the geodynamic setting of the Vandam zone during the Early Cretaceous period. To achieve this, petrographic and geochemical studies have focused on the siliciclastic rocks of the Kepuch and Gyrkhbulag Formations, which are well-exposed in the Vandam zone.

Geological setting and lithostratigraphy

The Kakheti-Vandam-Gobustan megazone corresponds to the northern flank of the South-Caucasian microplate with an Alpine cover composed of sedimentary and magmatogenic formations. From west to east, the Girdimanchay-Velvelychay flexure divides the megazone into two tectonically distinct zones. In the west, it is represented by the Vandam geoanticlinal uplift, where predominantly Cretaceous flysch deposits and volcanogenic formations are well exposed. Structurally this zone is composed of series of anticlines-synclines associated with several south directed thrusts. To the south, the Vandam zone is separated from Ganih-Ayricay zone by the fault of the same name. Most part of arch and southern slope of uplift is concealed under Pleistocene-Holocene continental formations of Ganih-Ayricay depression. In the east (interfluve of the Girdimanchay and Agsuchay rivers) the Mesozoic core of the Vandam uplift is flexurally downwarped along the Girdimanchay-Velvelyachay flexure and its southeastern continuation opens up into the wide Shamakhi-Gobustan depression, which is primarily composed of Paleocene-Pliocene terrigenous-clayey deposits. These deposits are folded into small, often overturned to the south sharp and isoclinal folds (Fig.1) (Alizadeh et al., 2005a).

Lithostragraphically the Neocomian deposits in the Vandam zone is divided into lithostratigraphic units based mostly on lithologic characteristics. These units include the Kepuch Formation followed by the Gyrkhbulag Formation in a sequence. The Lower Cretaceous deposits of the Vandam zone are characterized by slope facies sediments primarily composed of carbonate and siliciclastic turbidites. The lower part of the Kepuch Formation, represented by Berriasian deposits in the Vandam zone, is characterized by massive conglomerate layers interspaced with sections of limestones, marls, and tuffaceous sandstones.

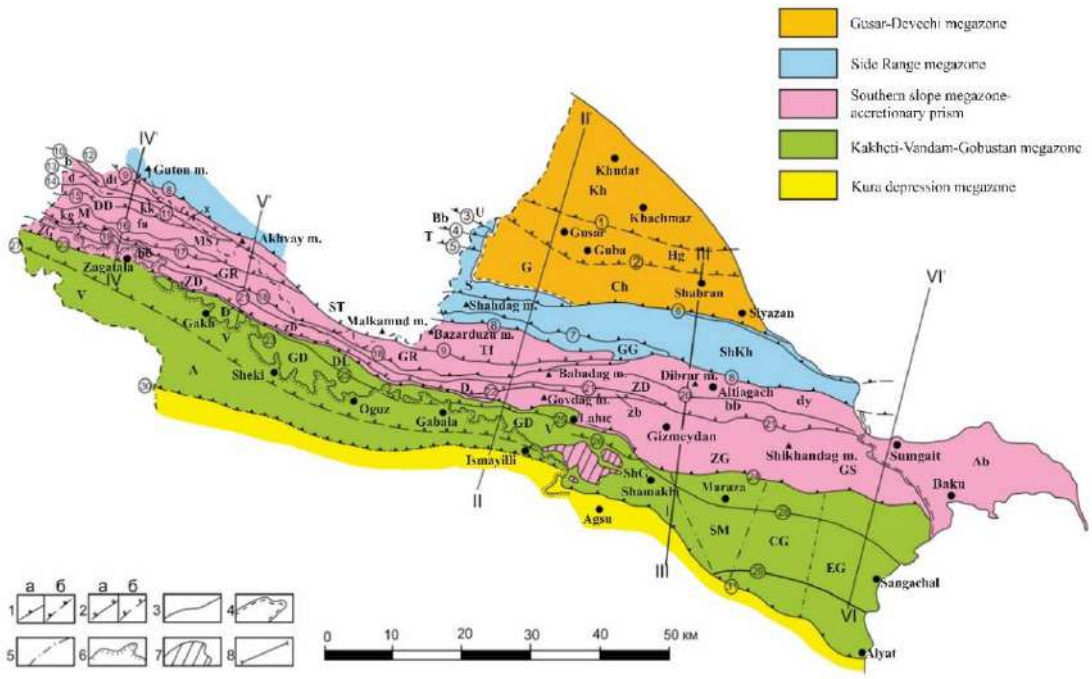

Fig. 1. Tectonic scheme of the Azerbaijani part of Greater Caucasus (Kangarli, 2012)

Boundary of strucrure: 1 – interzone tectonic boundaries (a – traced on surface; b – buried); 2 – tectonic boundaries between subzones (a – traced on surface; b – buried); 3 – boundaries of tectonic schuppens; 4 – stratigraphic boundaries; 5 – conventional boundaries; 6 – distribution boundary of modern sediements on Ganikh-Ayrichay superposed depression; 7 – Basgal nappe; 8 – lines of synthesized geological-geophisical sections

Structures: Gusar-Devechi megazone: zones: Kh – Xachmaz; G – Quba; subzones: Hg – Hasangala; Ch – Chilagir. Side Range megazone: zones: U– Ulluchay; Bb– Beybulag; T – Tairdjal; S – Sudur; ShKh – Shakhdag-Khizi; GG – Guton-Gonagkend. Southern Slope megazone: zones: ST – Speroz-Tufan; ZG – Zagatala-Govdag; Ab – Absheron; subzones: Tf – Tufan; DD – Djikhikh-Dindidag; MS – Mazim-Saribash; M – Megikan; GR – Galal-Rustambaz; ZD – Zagatala-Dibrar; D – Durudja; GS – Govdag-Sumqait; schuppens (nappe plates): dt – Djurmut-Tunsaribor; kh – Khalakhel; p – Rokhnor; b – Boskal; d – Djikhikh; кк – Kasdag-Kasmala; fa – Filizchay-Attagay; kg – Katekh-Gumbulchay; dy – Dibrar-Yashma; bb – Balakan-Babadag; zb – Zagatala-Burovdal. Kakheti-Vandam-Gobustan megazone: zones: V – Vandam; ShamG – Shamakhi-Gobustan; subzonesr: DL – Dashagil-Lahidj; GD – Gulluk-Dadagunash; A – Ayrichay; segments: Sh – Shamakhi; SM – Sundi-Maraza; CG – Central-Gobustan; EG – East-Gobustan

Fractures: 1 – İmamgulukend-Khachmaz; 2 – Khazra-Guba-Kuchay; 3 – Ashagimaki; 4 – Tendi-Keyda; 5 – Tairdjal; 6 – Siyazan; 7 – Shakhdag-Gonagkend; 8 – Major Caucasus; 9 – Khuray-Malkamud; 10 – Djoakhor-Gudurdag; 11 – Khalakhel; 12 – Kasmaldag; 13 – Machkhalor; 14 – Djikhikh-Chugak; 15 – Kokhnamadan; 16 – Hamzagor-Saribash; 17 – Suvagil; 18 – Gamarvan; 19 – Megikan; 20 – Altiagach; 21 – İlisu-Aladash; 22 – Gaynar-Gozluchay; 23 – Mamrux-Galadjig; 24 – Zangi-Garadjuzlu; 25 – Dashagil-Madrasa; 26 – Mudji; 27 – Shambul-İsmailli; 28 – Ganikh-Ayrichay; 29 – Adjichay-Alat

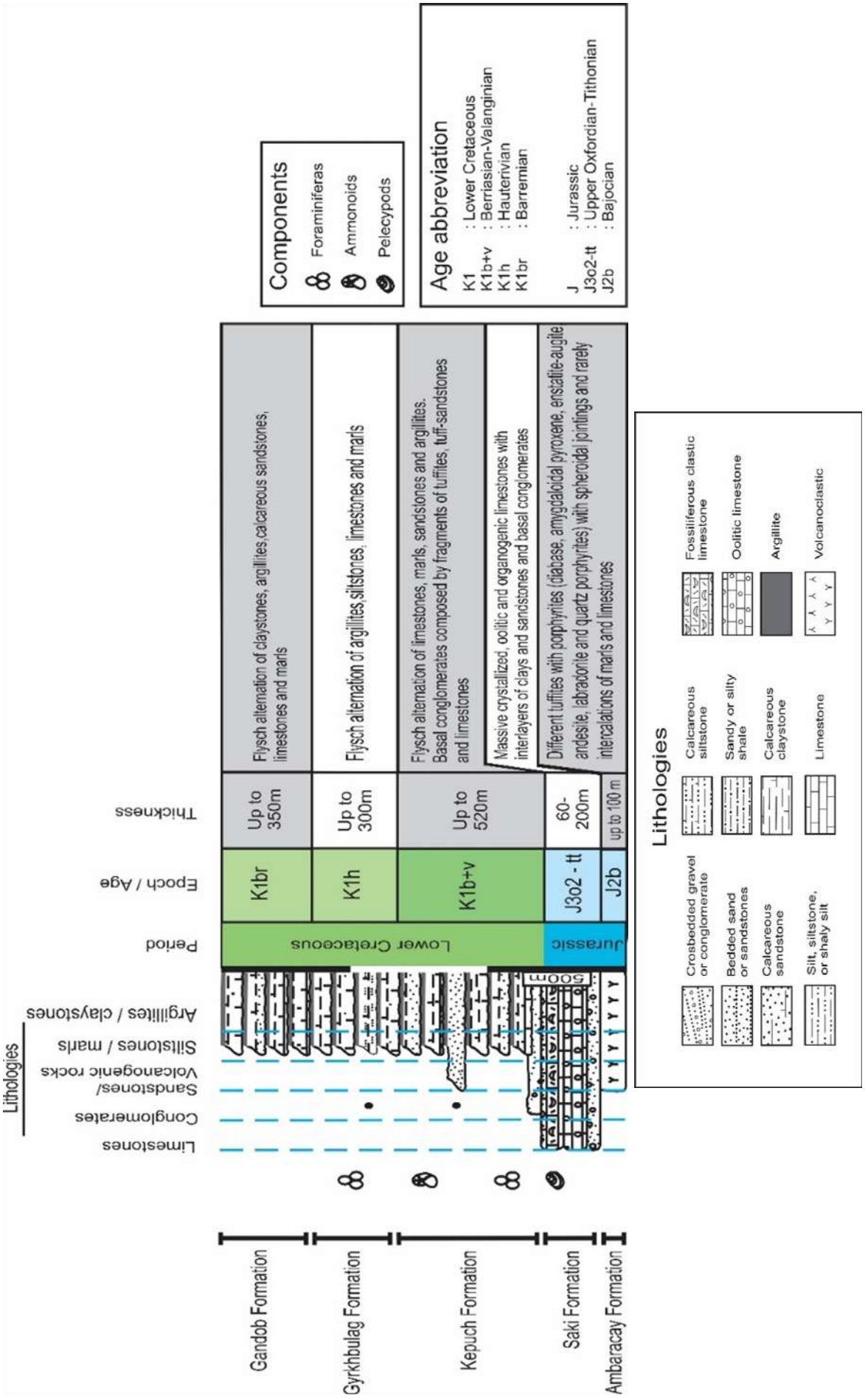

Fig. 2. Lithostratigraphic column of the Lower Cretaceous deposits of the Vandam zone (Alizadeh et al., 2005b)

The Valanginian deposits constitute the upper part of Kepuch Formation in the Vandam zone and are represented by a rhythmic alternation of grey, fine- to medium-grained calcareous sandstones and sandy limestones. In some places, pelitomorphic limestones alternate with marly clays and grey non-carbonate clays. The Hauterivian succession is comprised of terrigenous-carbonate flysch series and correspond to the Gyrkhbulag Formation. The thickness of these deposits reaches 300 m. These sediments are sharply different from the marly Kepuch Formation in their almost exclusively terrigenous character. The Hauterivian stage is dominated by argillites with interlayers of siltstones and sandstones. There are also individual interbeds of pelitomorphic limestone with a schistose structure (Alizadeh et al., 2005b) (Fig. 2).

Samples and methodology

In this study, ten samples were obtained from the Kepuch and Gyrkhbulag Formations, which are exposed in the Vandam zone on the southern slope of the Greater Caucasus. Sampling was conducted at five key outcrops: four riverbank locations along the Behmezchay (BC), Kishchay (KC), Damiraparanchay (DC), and Galachay (FL) rivers, and one roadside location (SQ) along the Sheki-Gakh route (Fig. 3). Initially, the samples were crushed for 20 minutes using a planetary ball mill to produce a homogeneous powder. This material was then further ground in a pulverizer. The fine powder (<100 μm) was placed in a porcelain crucible and subjected to drying at 1000°C overnight to eliminate moisture. Subsequently, the dried powder was combined with a binder (citric acid in a 1:10 ratio with the powder) and pulverized for an additional two minutes. This mixture was transferred into a 30 mm aluminum cap and compressed between two tungsten carbide pellets. A manual hydraulic press was used to apply a pressure of 10-15 tons per square inch for two minutes, followed by a gradual release of the pressure. The resulting compressed powder pellet was prepared for analysis. Major and trace elements were quantified via inductively coupled plasma mass spectrometry (ICP-MS) at the Laboratory of Geochemistry, Geochronology, and Isotope Geology, Department of Earth Sciences "Ardito Desio," at the Università degli Studi di Milano Statale, Italy.

For petrographic analysis, thin sections of ten representative samples were prepared at the geological laboratories of the University of Milano-Bicocca to assess mineralogical composition and microstructure. The unconsolidated samples were impregnated with epoxy resin, then cut and mounted on glass slides with Canada balsam. Slide preparation involved a three-stage grinding process, with inspections between each stage to ensure consistency in interference color reduction. The completed slides were labeled and examined under a petrographic microscope with a transmitted light and flat stage. Photomicrographs were captured to document mineral grain characteristics, which were analyzed based on their optical properties.

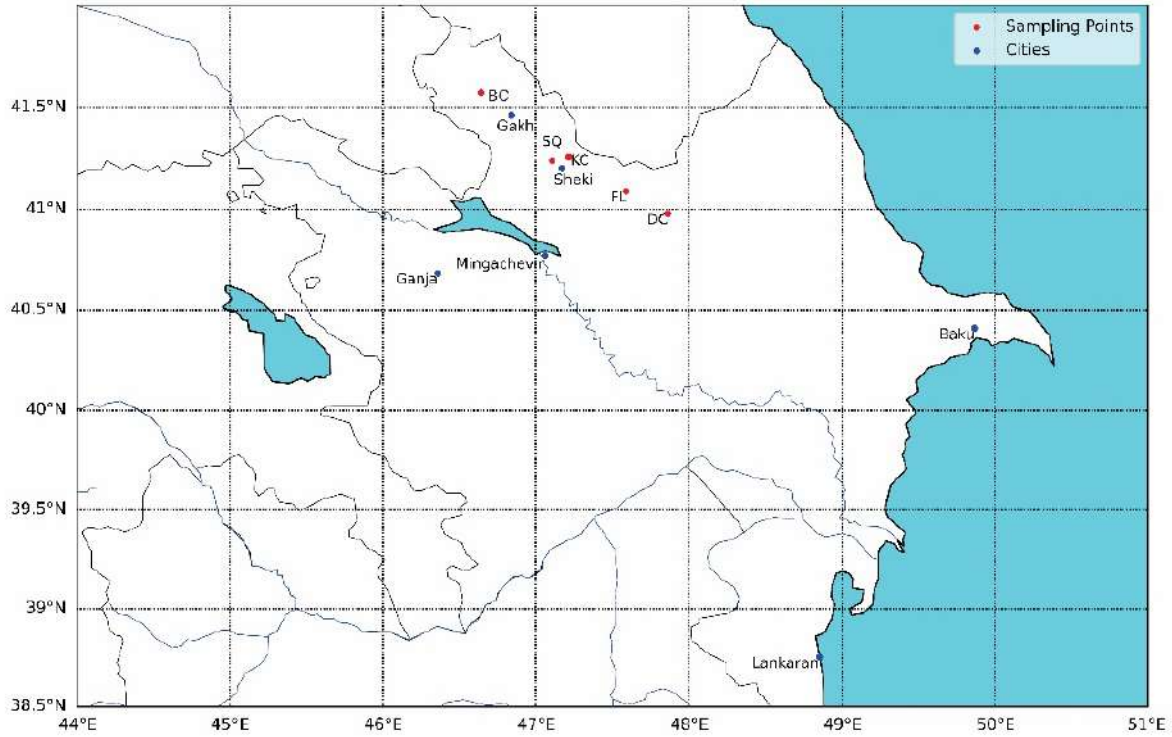

Fig. 3. Location map showing sampling points for the datasets used in the present work

Sandstone petrography

The sandstones analyzed are generally fine- to medium-grained. Microscopic examination of thin sections reveals that these sandstones comprise variable proportions of rock fragments, quartz, feldspars, matrix, and accessory minerals. The framework grains are predominantly composed of lithic clasts, with substantial contributions from quartz and feldspar (including both plagioclase and K-feldspar). Lithic fragments are primarily of volcanic (Lv) and metamorphic (Lm- quartz-mica lithic grain with schistosity) origin, with a minor component of sedimentary lithic fragments (Ls) (Fig. 4A, 4B, 4E). Volcanic lithic fragments (Lv) constitute the majority of the total lithic content. Quartz occurs mainly as monocrystalline grains, though polycrystalline quartz is also present in certain samples. Petrographic analysis reveals a lower proportion of K-feldspar relative to plagioclase (Fig. 4C). Majority of the samples contain varying proportions of mica, and muscovite (Fig. 4D) is more abundant than biotite since it is more resistant to weathering.

In accordance with the sandstone classification framework by (Pettijohn et.al.,1973), arenites are defined by a clay matrix content below 15%, whereas wackes are distinguished by a matrix exceeding 15%. As the matrix in the analyzed samples surpasses this 15% threshold and predominantly comprises clay minerals with minor detrital silts, these sandstones are classified as wackes. Furthermore, due to the dominance of lithic fragments within the framework grains, these sandstones are more precisely identified as lithic wackes. The cementing material is mainly authigenic calcite (Fig. 4F).

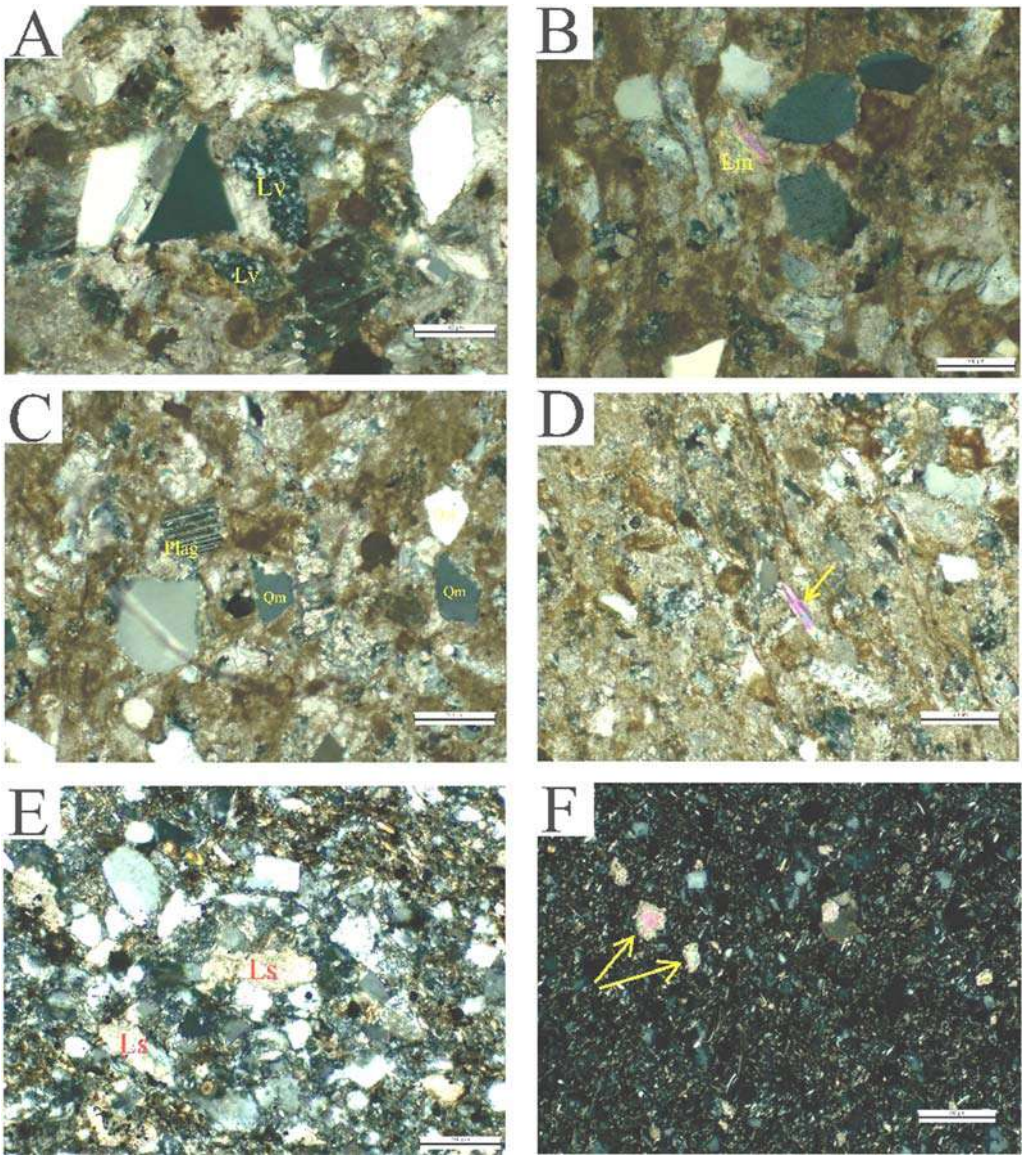

Fig. 4. Photomicrographs (in XPL) of thin-sectioned sandstones of the Kepuch and Gyrkhbulag formations showing: (A) felsic volcanic lithic fragment (Lv); (B) metamorphic lithic fragment (Lm); (C) angular to subangular monocrystalline quartz grains (Qm) and plagioclase (Plag); (D) detrital muscovite (yellow arrow) (E) sedimentary lithic fragment (Ls) (F) calcite cement (yellow arrows)

Geochemistry

Major elements

The major and trace element data are shown in Table 1 alongside average values of the Upper Continental Crust (UCC) for comparison (Taylor, McLennan, 1985). As shown in Table 1, the concentration of SiO_2 is high, varying between 55.61wt % and 79.27 wt % in the Kepuch Formation (KF), while it is between 60.33 wt% and 70.14 wt% in the Gyrkhbulag Formation (GF). The proportion of Al_2O_3 varies between 6.41wt% and 10.36 wt% in the KF, and 10.71-17.55 wt% in the GF. Compared to the upper continental crust (UCC), the SiO_2 and Al_2O_3 contents in the GF are the most similar to those of the UCC. Except for MnO and CaO, major element concentrations of samples from the KF are lower than the average values of the UCC (Fig.5). The samples from both formations are depleted in Na_2O, K_2O and P_2O_5. The GF that is distinguished by pronounced depletion in CaO (as is well seen in samples FL-1 and BC-1) have relatively high TiO_2 and FeO_2.

The K_2O/Al_2O_3 ratio in sandstone provides insight into the relative abundances of alkali feldspar and clay minerals prior to final burial. K-feldspar typically exhibits a K_2O/Al_2O_3 ratio as high as 0.9, while illite and kaolinite have lower ratios of approximately 0.3 and 0.04, respectively. (Cox et al., 1995). The low K_2O/Al_2O_3 ratios displayed by the KF and GF (0.18 and 0.16) are compatible with the predominantly illitic nature of these formations.

Trace elements and rare earth elements

Trace and rare earth element concentrations of the Kepuch and Gyrkhbulag formations are presented in Tables 1 and 2, respectively. Compared with average upper continental crust (UCC), the sandstones of the KF are characterized by relatively low concentrations of high field-strength elements (HFSE), whereas the concentrations of HFSE of rocks from the GF are close to UCC values (Fig.6). The distribution of Zr and Hf seems to be controlled by heavy mineral, such as zircon as indicated by the high correlation coefficient between Zr and Hf (r=0.97). This is supported by Zr/Hf ratios between 33 and 42, aligning well with those reported by Murali et al. (1983) for zircons.

The large ion lithophile elements (LILEs) are compared to UCC, among which Rb, Th and U are depleted in the KF samples. They are characterized by variable amounts of Ba and Sr. The samples of the GF exhibit a slight to strong depletion in Ba and Sr and minor enrichment in Cs and U (Fig.6). The siliciclastic rocks of both formations show a strong positive correlation between Rb and K_2O (r=0.99) indicating that Rb is mainly hosted by K-bearing clay mineral such as illite. In general, concentrations of transition trace elements (TTE) in the KF are lower than the average UCC concentrations. However, in a case study on the GF the average values of some TTE, such as Cr and Ni are comparable with those of UCC (Fig.6).

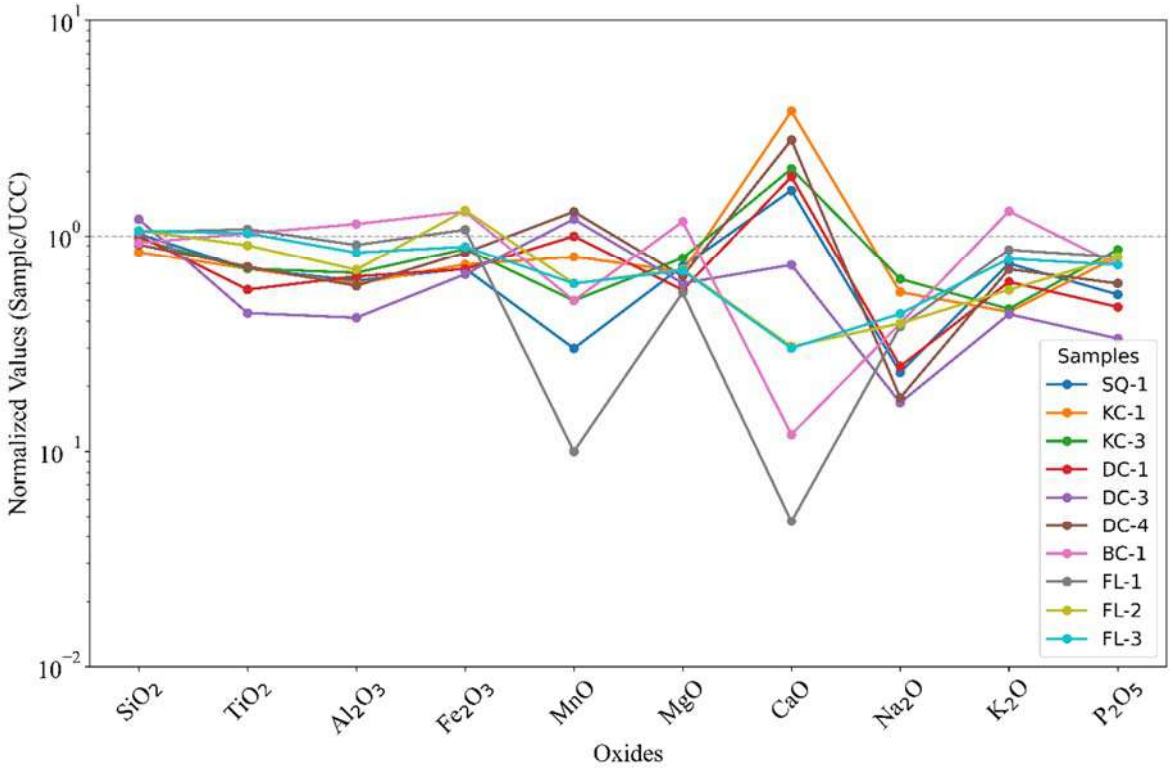

Fig. 5. Spider plot of major elements in Lower Cretaceous (Neocomian) deposits normalized against UCC (upper continental crust)

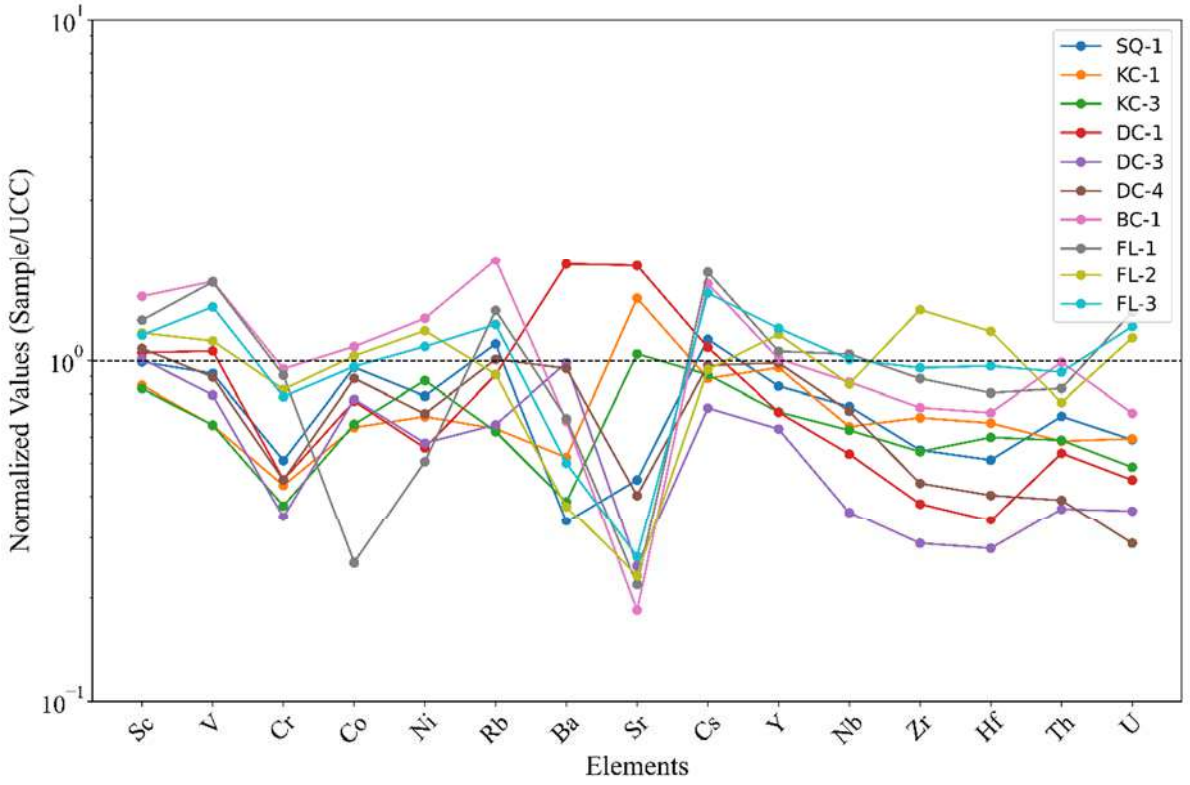

Fig. 6. Spider plot of trace element concentrations in Lower Cretaceous (Neocomian) deposits normalized against UCC (upper continental crust)

Table 1

Major (wt%) and trace element (ppm) concentrations of the samples from the Kepuch and Gyrkhbulag Formations

Formation	Kepuch Formation						Gyrkhbulag Formation					
Sample no.	SQ-1	KC-1	KC-3	DC-1	DC-3	DC-4	BC-1	FL-1	FL-2	FL-3	UCC	PAAS
SiO_2	67.70	55.61	63.82	66.33	79.27	60.33	61.41	68.69	70.14	69.98	65.89	62.9
TiO_2	0.45	0.45	0.45	0.36	0.28	0.46	0.66	0.69	0.58	0.66	0.50	0.99
Al_2O_3	9.52	9.24	10.36	9.97	6.41	9.02	17.55	14.02	10.71	12.91	15.17	18.9
Fe_2O_3	3.55	3.71	4.39	3.53	3.34	4.22	6.56	5.40	6.65	4.50	4.49	7.22
MnO	0.03	0.08	0.05	0.10	0.12	0.13	0.05	0.01	0.06	0.06	0.07	0.11
MgO	1.79	1.69	1.96	1.39	1.49	1.61	2.90	1.35	1.73	1.71	2.20	2.20
CaO	5.86	13.64	7.38	6.78	2.63	10.04	0.43	0.17	1.10	1.08	4.19	1.29
Na_2O	0.76	1.79	2.06	0.81	0.55	0.58	1.28	1.24	1.28	1.42	3.89	1.18
K_2O	2.08	1.24	1.28	1.71	1.21	1.96	3.66	2.42	1.57	2.19	3.39	3.70
P_2O_5	0.08	0.12	0.13	0.07	0.05	0.09	0.11	0.12	0.12	0.11	0.20	0.16
LOI	8.17	12.42	8.12	8.95	4.66	11.58	5.38	5.88	6.06	5.37	-	-
Sc	13.90	11.87	11.60	14.79	14.19	15.20	21.63	18.40	16.89	16.63	13.6	16
V	89.09	62.90	63.03	103.56	77.02	86.99	165.83	165.13	110.82	139.50	107	130
Cr	47.05	39.74	34.60	41.36	32.05	41.25	87.16	83.44	75.89	72.27	85	110
Co	16.56	11.06	11.30	13.20	13.38	15.36	19.03	4.39	17.87	16.65	17	23
Ni	37.08	32.32	41.16	26.19	27.06	32.95	62.53	23.87	57.53	51.74	44	55
Cu	14.54	15.02	17.01	61.98	34.78	64.19	47.25	48.51	44.84	45.35	25	50
Zn	55.56	60.61	75.53	65.52	53.22	57.47	134.38	63.80	138.38	90.05	71	85
Rb	94.07	53.26	52.23	76.49	54.70	84.83	166.17	117.91	76.75	107.27	112	160
Sr	143.40	488.02	335.03	609.42	79.39	129.09	59.02	70.28	74.54	84.57	350	200
Zr	106.00	131.73	104.84	73.50	55.78	84.60	141.06	171.22	272.17	184.02	190	210
Cs	5.66	4.35	4.46	5.36	3.57	4.75	8.25	8.92	4.62	7.74	4.6	9.3
Ba	211.74	328.01	242.46	1208.43	619.72	596.55	418.54	426.20	234.42	315.47	550	650
Pb	15.14	12.13	14.36	13.69	8.33	25.46	28.66	19.26	15.63	20.34	17	20
Th	7.23	6.12	6.16	5.64	3.86	4.10	10.40	8.72	7.94	9.73	10.7	14.6
U	1.59	1.60	1.32	1.21	0.98	0.78	1.90	3.75	3.15	3.40	2.8	3.1

The TTE show a slight enrichment of Sc and V for the GF. For the GF samples, Al_2O_3 exhibits a significant positive correlation with Sc and V (r=0.93 and r=0.86, n=4 respectively), indicating phyllosilicates as a major controlling factor for V and Sc concentrations.

The total Rare Earth Elements (∑REE) in KF ranges from 65.86 to 105.43 ppm (mean = 85.80 ppm) while in GF it varies from 115.05 ppm to 132.94 ppm (mean = 123.73 ppm). If normalized to chondrite values (Fig.7), both Kepuch and Gyrkhbulag samples exhibit enrichment in LREE (La_{cn}/Sm_{cn}; 2.38-3.37 and 2.79-3.89) and have an almost flat HREE (Gd_{cn}/Yb_{cn}; 1.18-1.86 and 1.05-1.55, respectively) patterns with a negative Eu anomaly (Eu/Eu* = 0.69–0.75 for KF, and 0.63-0.73 for GF). Eu anomalies were calculated as $Eu/Eu^*=(Eu)_{cn}/[(Sm)_{cn} \times (Gd)_{cn}]^{0.5}$ (McLennan 1989), where cn expresses chondrite-normalized values of the element (Taylor and McLennan 1985). The values of ∑LREE/∑HREE are variable and range from 6.05 to 7.93, where the average value is 6.97.

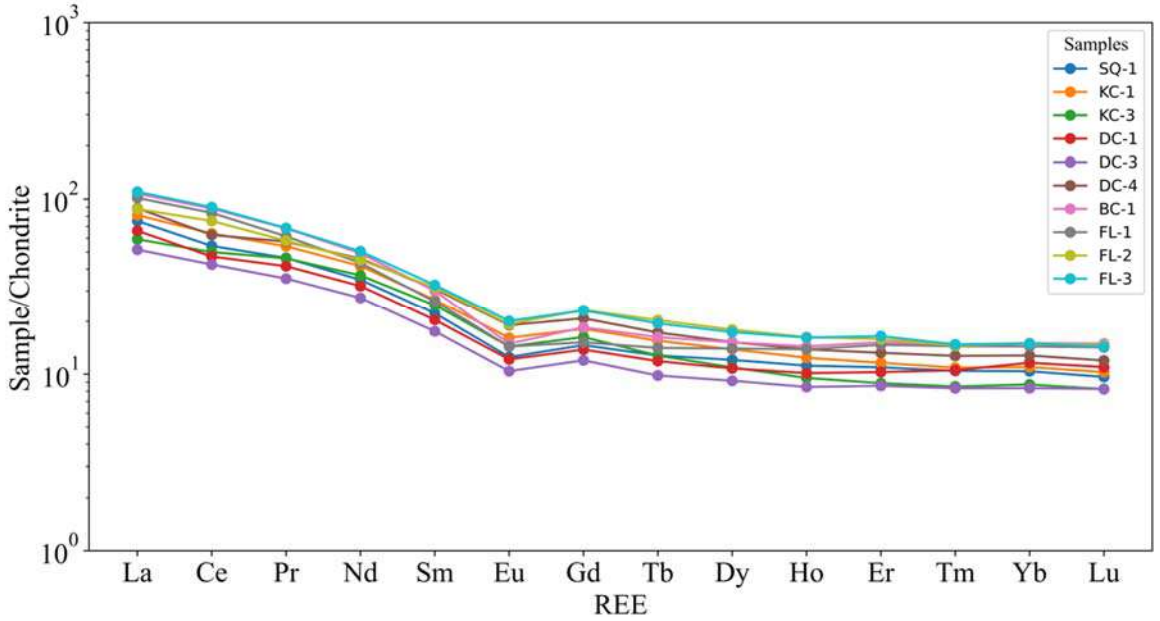

Fig.7 Chondrite-normalized rare earth elements plot for Lower Cretaceous (Neocomian) deposits of Vandam zone

Table 2

Rare earth element concentrations (ppm) of the samples from Kepuch and Gyrkhbulag Formations

Formation	Kepuch Formation						Gyrkhbulag Formation				
Sample №	SQ-1	KC-1	KC-3	DC-1	DC-3	DC-4	BC-1	FL-1	FL-2	FL-3	Chondrite Values
La	17.82	19.24	14.03	15.68	12.24	21.05	25.46	24.12	20.86	26.11	0.237
Ce	33.24	39.12	30.69	28.95	26.06	38.42	54.24	51.27	46.12	55.22	0.613
Pr	4.30	5.02	4.28	3.86	3.28	5.33	6.34	5.71	5.39	6.36	0.0928
Nd	15.88	19.04	16.82	14.63	12.51	20.96	22.53	19.83	20.62	23.11	0.457
Sm	3.30	3.96	3.68	3.02	2.60	4.57	4.45	3.86	4.67	4.80	0.148
Eu	0.70	0.91	0.81	0.68	0.59	1.07	0.84	0.81	1.08	1.13	0.0563
Gd	2.91	3.61	3.24	2.75	2.38	4.14	3.68	3.02	4.63	4.59	0.199
Tb	0.46	0.56	0.46	0.43	0.35	0.62	0.59	0.51	0.73	0.70	0.0361
Dy	2.96	3.41	2.69	2.65	2.26	3.74	3.74	3.44	4.41	4.27	0.246
Ho	0.61	0.68	0.52	0.55	0.46	0.76	0.79	0.76	0.89	0.88	0.0546
Er	1.75	1.86	1.42	1.64	1.37	2.12	2.43	2.35	2.53	2.63	0.16
Tm	0.26	0.27	0.21	0.26	0.21	0.31	0.36	0.36	0.36	0.36	0.0247
Yb	1.67	1.77	1.41	1.87	1.34	2.06	2.42	2.32	2.41	2.41	0.161
Lu	0.24	0.25	0.20	0.27	0.20	0.29	0.37	0.35	0.36	0.35	0.0246

Results and discussion

Geochemical Classification

Pettijohn et al. (1972) and Herron (1988) established classification frameworks that utilize geochemical characteristics to categorize sedimentary rocks. Utilizing the classification diagram from Herron (1988) (Fig. 8A), it was determined that most of the analyzed samples are situated within the wacke classification field, indicating a degree of immaturity. In accordance with the classification scheme proposed by Pettijohn et al. (1972), as illustrated in Figure 8B, the studied samples are predominantly classified as litharenites, with a minority being classified as arkoses.

Inferences on Paleoweathering

Chemical weathering is a key process influencing interelemental fractionation, leading to elemental ratios that differ from those in the source rocks. The intensity and extent of chemical weathering in clastic rocks can be assessed through various indices, including the Chemical Index of Alteration (CIA), Plagioclase Index of Alteration (PIA), and Chemical Index of Weathering (CIW) (Nesbitt and Young, 1982, 1984; Fedo et al., 1995; Harnois, 1988).

The Chemical Index of Alteration (CIA), introduced by Nesbitt and Young (1982), is one of the most widely used indicators of chemical weathering. Higher CIA values correlate with increased chemical weathering and a higher presence of residual clay minerals, such as illite, chlorite, kaolinite, and gibbsite. High CIA values signify intense weathering or sediment recycling, often under warm, humid paleoclimatic conditions, which results in the depletion of soluble cations (Ca^{2+}, Na^{+}, K^{+}) favor of less soluble cations like Al^{3+} and Ti^{4+}. In contrast, low CIA values reflect limited or negligible chemical weathering, generally associated with cool or arid climates. The CIA is expressed as CIA= $[Al_2O_3/(Al_2O_3+CaO+ Na_2O+K_2O)]x100$, where Al_2O_3, CaO, Na_2O, and K_2O are in molar proportions, and CaO* incorporated in silicate fraction of sediments. The CIA excludes the influence of carbonate minerals, thus reflecting the weathering intensity of silicate minerals and providing insights into the chemical weathering conditions in the source area. For the samples in this study, CIA values ranging from 55.9 to 73.7 suggest a weak to moderate degree of chemical weathering in the source rocks.

CIA values can be plotted on a Al_2O_3-(CaO+ Na_2O)-K_2O (A-CN-K) ternary diagram to refine assessments of weathering processes and evaluate potential K-metasomatism effects more precisely. This diagram also facilitates the delineation of the primary geochemical composition of the source rocks (Nesbitt and Young, 1982, 1984; Fedo et al., 1995). In this study, the samples plot along the weathering trend for granodioritic compositions, progressing towards illite without any detectable influence of K-metasomatism (Fig. 9).

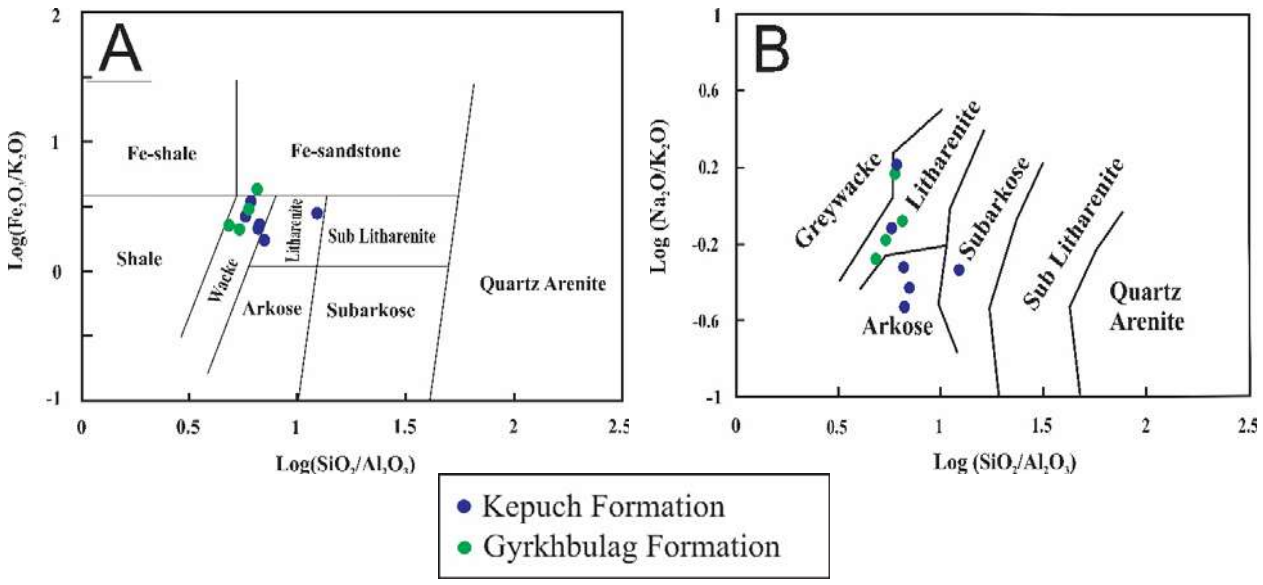

Fig. 8. Geochemical classification of samples (A) log ratios of SiO_2/Al_2O_3 – Fe_2O_3/K_2O (Herron, 1988); (B) log ratios of SiO_2/Al_2O_3 – Na_2O/K_2O (Pettijohn et al., 1972)

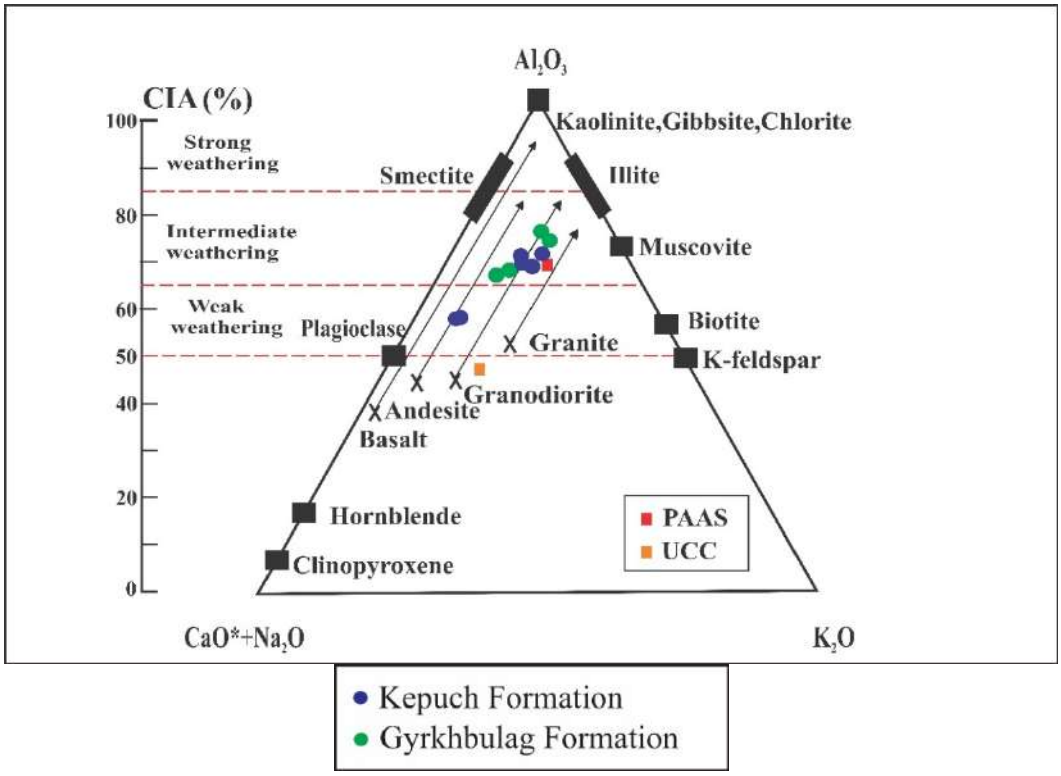

Fig. 9. The A-CN-K ternary plot of the samples; Al, Al_2O_3; CN, CaO* + Na_2O; K, K_2O (oxides are plotted as molar); (PAAS-Post-Archean Australian Shale; UCC-Upper Continental Crust)

The extent of weathering can also be assessed by analyzing the molecular percentages of oxide components using the Chemical Index of Weathering (CIW), as proposed by Harnois (1988). Like the CIA, the CIW gauges the degree of chemical weathering and the alteration of feldspar to clay minerals (Nesbitt and Young, 1984, 1989; Fedo et al., 1995; Maynard et al., 1995). It is defined as: $CIW=[Al_2O_3/(Al_2O_3+CaO^*+Na_2O]x100$, where Al_2O_3, CaO, and Na_2O are in molar proportions and CaO* is restricted to the amount of CaO in the silicate fraction only. The CIW calculation resembles that of CIA but omits K_2O, accounting for the possible leaching or retention of potassium in weathering products during sedimentation. Due to its higher cation exchange capacity, potassium is more easily incorporated into clay minerals compared to Na^+ and Ca^+ (Kroonenberg, 1994). This exclusion of K_2O minimizes complications associated with K mobilization during diagenesis or metamorphism. CIA and CIW values are interpreted similarly, with values around 50 indicating unweathered upper continental crust and values near 100 reflecting highly weathered materials (e.g., kaolinite and gibbsite). The CIW values for the samples, ranging from 60 to 85 with an average of 75, indicate low to moderate levels of weathering in the source materials, aligning with the CIA.

The Plagioclase Index of Alteration (PIA), developed by Fedo et al. (1995), serves as an alternative to the Chemical Index of Weathering (CIW), targeting specifically the alteration of plagioclase feldspar, a prevalent mineral in silicate rocks. This index is particularly useful when the focus is on assessing plagioclase weathering independently. An unweathered plagioclase has a PIA value of 50, while a fully weathered material reaches a maximum value of 100. The PIA is calculated using the formula:

$$PIA=[(Al_2O_3-K_2O)/(Al_2O_3+CaO^*+Na_2O-K_2O)]x100,$$

where CaO* represents only the CaO bound within the silicate fraction, and all oxide quantities are expressed in moles. For the samples examined, PIA values ranged from 56.9 to 82.8, with an average of 72.1, indicating a low to moderate degree of chemical weathering.

Implications for provenance

Various discrimination diagrams on the basis of the major-element compositions of clastic rocks have been established in order to infer their provenance characteristics. The major-element-based provenance discrimination functions diagram, introduced by Roser and Korch (1988), was applied to discriminate the source area into four major prove-

nance fields. They are the mafic igneous (P1), intermediate igneous (P2), felsic igneous (P3) and quartzose sedimentary or recycled (P4). As can be noted from discrimination plot all data lie in the fields of intermediate igneous provenance and quartzose sedimentary provenance, implying mixed source area (Fig.10A).

Additionally, since Al, Ti, and Zr oxides and hydroxides exhibit low solubility, they are often considered immobile elements; as a result, the Al_2O_3/TiO_2 ratio in the samples closely matches that of their source rocks. The Al_2O_3/TiO_2 ratio values range from 3 to 8 for mafic rocks, 8 to 21 for intermediate rocks, and 21 to 70 for felsic igneous rocks, providing insights into the source area composition (Schieber, 1992). The Al_2O_3/TiO_2 ratio of the analyzed samples varies from 18.46 to 27.69, with an average of 22.03, which is in agreement with felsic to intermediate source rock (Fig.10B). In addition, the bivariate Al_2O_3 versus TiO_2 diagram shows a concentration of data in the felsic rock field, and only few samples plot within the field for intermediate igneous rocks. This analysis is supported by the bivariate plot of K_2O versus Rb (Fig.10C), which shows that source rocks of samples are felsic to intermediate igneous source rocks (Floyd et.al., 1989).

Apart from the major elements, trace element compositions and REEs can be used to judge the sediment provenance and the source-area rock composition due to their relatively immobile behaviour in the sedimentary environment. La/Th ratios in clastic sedimentary rocks are regarded as a powerful tool for reconstructing the source composition of sediments, while Hf concentration of a sediment typically reveals the degree of recycling that has occurred (Floyd et.al., 1987). In a cross-plot of La/Th versus Hf, apart from two metapsammite samples plotted within the andesitic arc source field, most analysed samples are characterized by low Hf content (1.48-6.46 ppm) and La/Th ratios (typically less than 3.5 ppm) plotting within the mixed felsic/basic source field (Fig.10D).

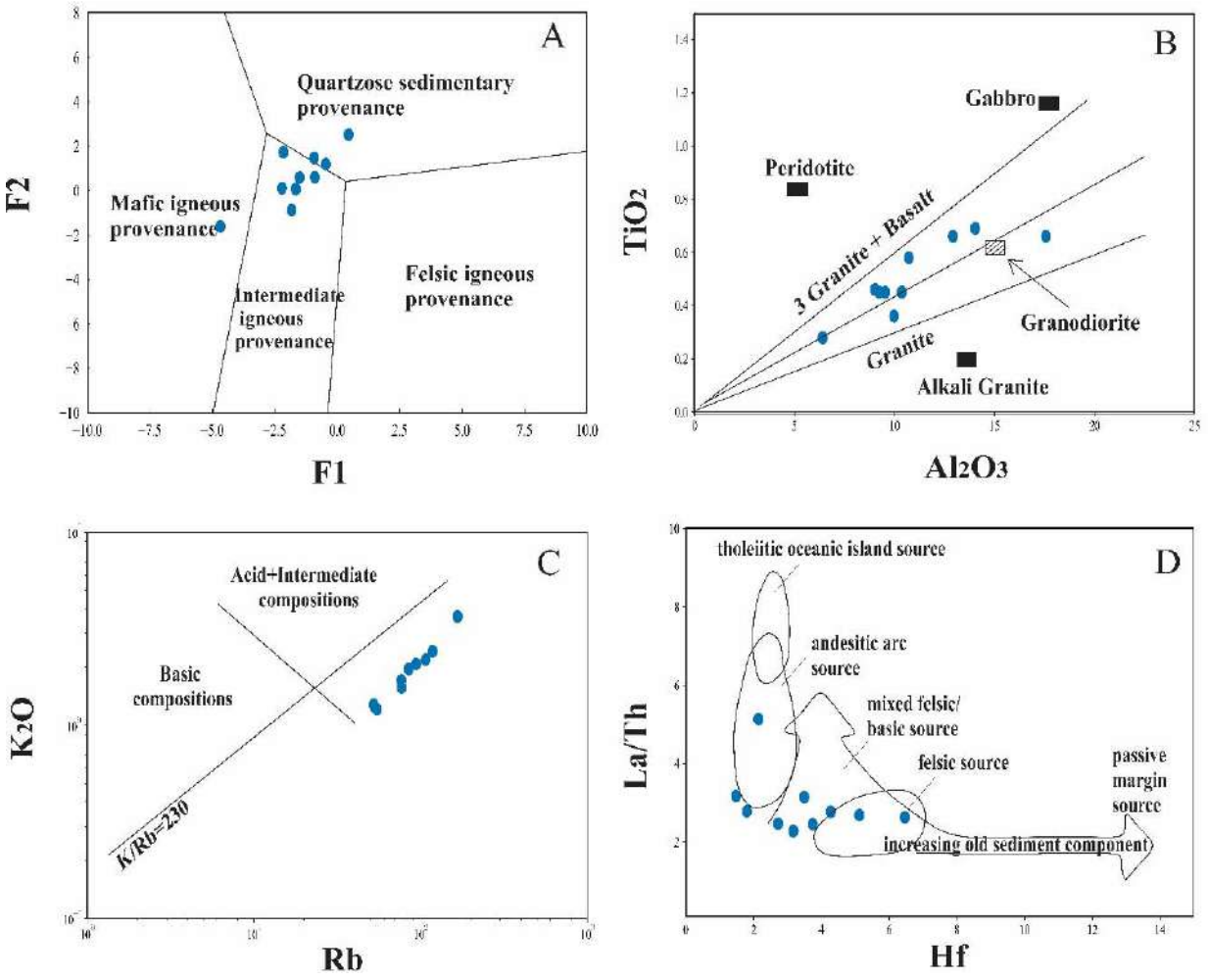

Fig.10. A) Sediment provenance diagram using major element discriminant function analysis after (Roser and Korsch, 1986) **B)** Provenance diagram of Al_2O_3 versus TiO_2 after (Schieber,1992) **C)** The K_2O vs Rb diagram (Floyd & Leveridge 1987; Floyd et al., 1990) **D)** Binary plot of Hf vs. La/Th showing the provenance of the studied sediments (fields after Floyd and Leveridge, 1987)

Tectonic Setting

The distribution of major, trace, and rare earth elements in sedimentary rocks serves as a robust tool for elucidating the nature of their tectonic environment, as distinct geochemical characteristics are often associated with specific plate tectonic environments. Roser and Korsch (1986) have proposed a tectonic discrimination diagram based on bivariate plot of SiO_2 versus K_2O/Na_2O in order to define tectonic setting of terrigenous sedimentary rocks. Figure 11A shows that majority of samples plotted in the field of active continental margin. Active continental margin setting described by Roser and Korsch suggests that sediments were derived from subduction-related basins formed in continental arcs or strike-slip basins along convergent margins.

The major element-based discriminant function diagrams of Bhatia (1983) are divided into four different fields such as oceanic island arc (OIA), continental island arc (CIA), active continental margin (ACM), and passive margin (PM). On multi-parametric major-element based discriminant function diagram (Fig.11B) developed by Bhatia (1983), samples falls on active tectonic setting field. Tests on known samples showed that there is a marked increase in Fe_2O_3*+MgO and Al_2O_3/SiO_2 as the tectonic setting changes in the following sequence: PM-ACM-CIA-OIA (Bhatia, 1983). On the Al_2O_3/SiO_2 versus Fe_2O_3+MgO discrimination diagram (Bhatia 1983), most of analysed samples fall within continental island arc field (CIA) (Fig. 11C).

Moreover, elements La, Th, Zr, Nb, Y, Sc, Hf, Co and Ti are also very useful in tectonic setting discrimination because of their strong stability and high discriminating strength. La–Th–Sc discrimination diagram after Bhatia (1983) reveals that most of samples have the characteristics of a continental island arc as expected, which is in good agreement with major element tectonic discrimination (Fig. 12). In the bivariate Ti/Zr versus La/Sc plot after Bhatia and Crook (1986), once again most of the samples are found to concentrate on the continental island arc environment (Fig. 11D).

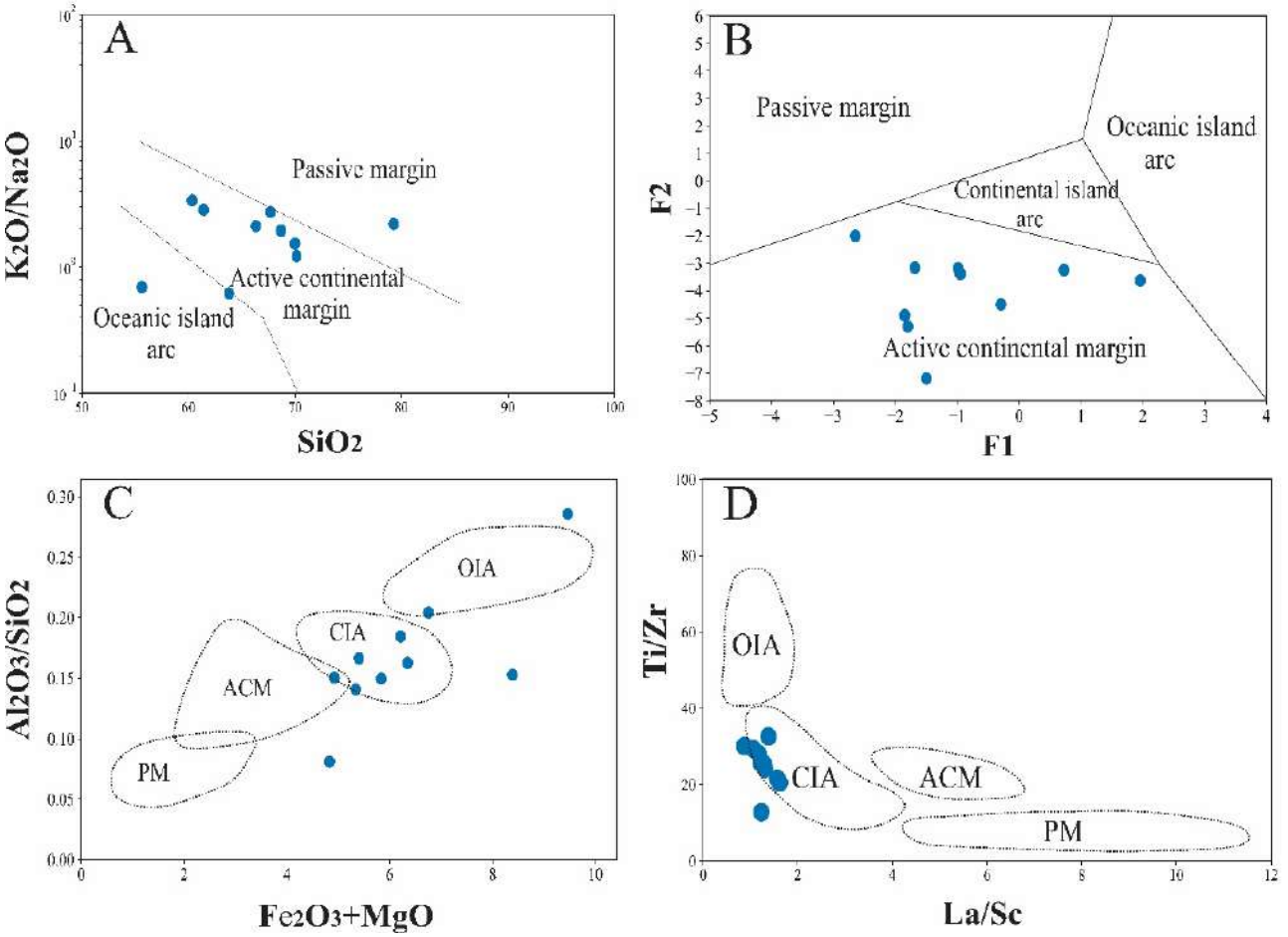

Fig.11 A) The K_2O/Na_2O vs. SiO_2 discrimination diagram (Roser and Korsch, 1986) showing tectonic setting fields for Neocomian deposits of Vandam zone **B)**$discriminant function diagram of Bhatia (1983) **C)** Tectonic setting diagram a Fe_2O_3 + MgO vs. Al_2O_3/SiO_2 after Bhatia (1983) **D)** Discrimination plot La/Sc vs. Ti/Zr for tectonic settings (Bhatia and Crook, 1986)

Similarly, more detailed results can be obtained using Eu/Eu*–La_N/Yb_N diagram after McLennan (1993). In this diagram depicted in Figure 13, the La_N/Yb_N ratio varies within the range of 5.88 to 9.26, and the Eu/Eu* value of most samples is less than 0.85, indicating that most sample parameters in this area are within the continental island arc tectonic setting.

According to Bhatia (1985), the chondrite normalized patterns of continental island arc-derived sediments are characterized by moderate enrichment of LREE relative to HREE accompanied by slight negative anomaly of Eu (mean Eu/Eu*=0.79). Applying these parameters to the analysed samples (Fig. 7), their REE characteristics indicate a strong match with a continental island arc environment.

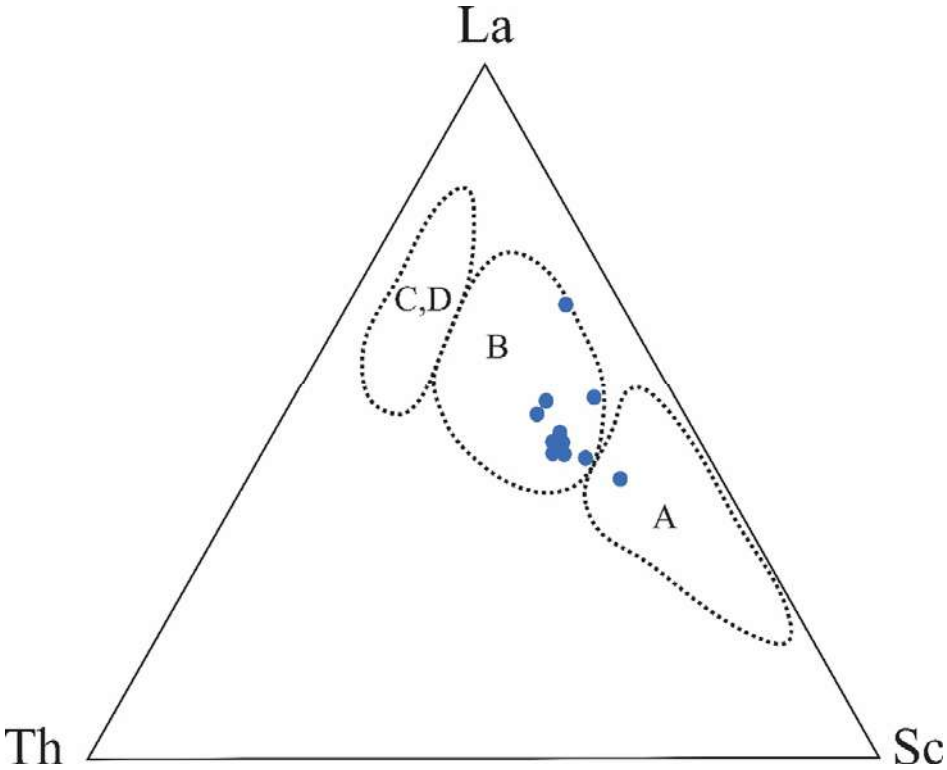

Fig. 12. Discrimination plots La-Th-Sc and Th-Sc-Zr/10 for tectonic settings (Bhatia and Crook, 1986). The tectonic regimes active (C) and passive (D) continental margins and continental (B) and oceanic (A) island arcs are distinct

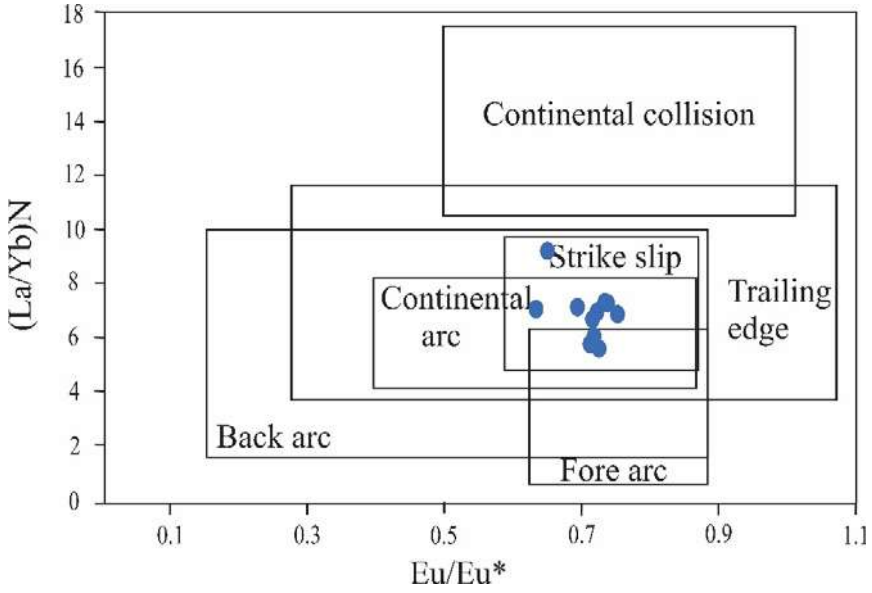

Fig. 13. Eu/Eu* versus LaN/YbN diagram after McLennan et al. (1993) showing samples clustering within the continental island arc region. The Eu/Eu* is computed using the equation $Eu/Eu^*=(Eu)_{cn}/[(Sm)_{cn} \times (Gd)_{cn}]^{0.5}$, where "cn" represents the values of each element normalized to chondrite

Conclusion

The analyzed samples are categorized as wackes and litharenites according to geochemical classification diagrams. However, since the matrix content exceeds 15%, they are more precisely classified as greywackes.

The Chemical Index of Alteration (CIA) values for the analyzed sandstones vary from 55.9 to 73.7, suggesting a low to moderate extent of chemical weathering in their source regions. Additionally, the ratios of the Chemical Index of Weathering (CIW) and the Plagioclase Index of Alteration (PIA) further indicate that the sediments in the source areas underwent low to moderate weathering before being deposited in the basin. The A-CN-K diagram further defines the primary composition of the source rocks, revealing that the analyzed samples align with the ideal weathering trend for granodiorite toward an illite composition, without indicating any evidence of K-metasomatism.

The analysis of provenance suggests that the sandstones originate from a mixed source area, primarily composed of intermediate igneous rocks, as indicated by major-element discrimination diagrams. Additionally, trace element ratios like La/Th and Hf concentrations reinforce the notion that the source rocks are predominantly felsic to intermediate, with minimal signs of recycling.

The geochemical analysis of major, trace, and rare earth elements in the studied siliciclastic rocks strongly suggests a provenance linked to a continental island arc tectonic setting. Discriminant diagrams, including the SiO_2–K_2O/Na_2O plot by Roser and Korsch and the Al_2O_3/SiO_2 versus Fe_2O_3+ MgO diagram by Bhatia, robustly position the samples within fields characteristic of active continental margins and continental island arcs, indicating a subduction-influenced sediment source. Additionally, the La–Th–Sc ternary diagram and Ti/Zr versus La/Sc bivariate plot provide further evidence, with most samples aligning closely with continental island arc signatures. The Eu/Eu*–La_N/Yb_N plot reveals rare earth element patterns that are emblematic of sediments derived from a continental island arc setting. Altogether, these geochemical indicators emphasize the significant influence of tectonic processes on the composition of the studied siliciclastic rocks, underscoring their tectonic heritage.

These results exhibit a strong correlation with the geodynamic interpretation of the region, as demonstrated by the works of R.N. Abdullayev and M.I. Rustamov, thereby enhancing our understanding of the tectonic dynamics involved. According to M.I. Rustamov, at the onset of the Jurassic, rifting and uncompensated subsidence initiated along the boundary between the Scytho-Turanian and South Caucasian plates, characterized by spreading in the Goitkh-Tfan trough. This area, extending from Crimea to the Absheron threshold, exhibited a distinct pattern of rift-related magmatism, including intrusive bodies and basalt flows. During the pre-Bajocian phase, diffuse spreading ceased, marking a shift to an Andean-style margin of the Scythian Plate. At this critical stage of compression, aspido-slate complex with magmatic bodies in the axial trough of the Greater Caucasus transforms into an accretionary prism, augmenting the active Scythian margin and zones of differentiated magmatism. The increasing compression phase led to southward subduction, resulting in the formation of the Kakheti-Vandam and Gagra-Dzhava zones as sites for continental island-arc volcano-plutonic associations. The Late Jurassic-Neocomian period marked the culmination of late Kimmerian tectogenesis, characterized by granitoid intrusions and the stabilization of the compressional geodynamic setting.

REFERENCES

Abdullaev R.N., Mustafaev M.A., Samedova R.A., Shafiev Kh.I., Mamedov M.N. Petrology of Magmatic Complexes of the Southern Slope of the Greater Caucasus (Vandamskaya Zone). Elm. Baku. 1990 (in Russian).

Alizadeh Ak.A. (ed.). Geology of Azerbaijan. Volume 4: Tectonics. Nafta Press. Baku, 2005a, 580 p. (in Russian).

Alizadeh Ak.A. (ed.). Geology of Azerbaijan. Volume 1: Stratigraphy. Nafta Press. Baku, 2005b, 580 p. (in Russian).

Bhatia M.R. Plate tectonics and geochemical composition of sandstone. The Journal of Geology, Vol. 91,1983, pp. 611-627, http://dx.doi.org/10.1086/628815

Bhatia M.R., Crook K.A.W. Trace element characteristics of graywackes and tectonic setting discrimination of sedimentary basins. Contributions to Mineralogy and Petrology, Vol. 92(2), 1986, pp. 181-193, https://doi. org/10.1007/BF00375292.

Cox R., Lowe D.R., Cullers R.L. The influence of sediment recycling and basement composition on evolution of mudrock chemistry in the Southwestern United States. Geo-

ЛИТЕРАТУРА

Абдуллаев Р.Н., Мустафаев М.А., Самедова Р.А., Шафиев Х.И., Мамедов М.Н. Петрология магматических комплексов южного склона Большого Кавказа (Вандамская зона). Элм. Баку, 1990, 204 с.

Ализаде Ак.А (под ред.). Геология Азербайджана. Том 4: Тектоника. Нафта Пресс. Баку, 2005a, 580 с.

Ализаде Ак.А (под ред.). Геология Азербайджана. Том 1: Стратиграфия. Часть 2: Мезозойская и кайнозойская эры. Нафта Пресс. Баку, 2005a, 580 с.

Рустамов М.И. Геодинамика и магматизм Загрос-Кавказского сегмента в фанерозое. Palmarium Academic Publishing. 2016, 543 с.

Bhatia M.R. Plate tectonics and geochemical composition of sandstone. The Journal of Geology, Vol. 91,1983, pp. 611-627, http://dx.doi.org/10.1086/628815

Bhatia M.R., Crook K.A.W. Trace element characteristics of graywackes and tectonic setting discrimination of sedimentary basins. Contributions to Mineralogy and Petrology, Vol. 92(2), 1986, pp. 181-193, https://doi. org/10.1007/BF00375292.

chimica et Cosmochimica Acta, Vol. 59, No. 14, 1995, pp. 2919-2940, https://doi.org/10.1016/0016-7037(95)00185-9.

Fedo C.M., Nesbitt H.W., Young G.M. Unravelling the effects of potassium metasomatism in sedimentary rocks and paleosols, with implications for palaeo-weathering conditions and provenance. Geology, Vol. 23, No. 10, 1995, pp. 921-924, https://doi.org/10.1130/0091-7613(1995)023<0921: UTEOPM>2.3.CO;2.

Floyd P.A. and Leveridge B.E. Tectonic environment of the Devonian Gramscatho Basin South Cornwall: Framework mode and geochemical evidence from turbiditic sandstones. Journal of the Geological Society (London), Vol. 144, 1987, pp. 531-542, http://dx.doi.org/10.1144/gsjgs.144.4.0531.

Floyd P.A. and Leveridge B.E. Tectonic environment of the Devonian Gramscatho Basin South Cornwall: Framework Mode and Geochemical Evidence from Turbiditic Sandstones. Journal of the Geological Society (London), Vol. 144, 1987, pp. 531-542, http://dx.doi.org/10.1144/gsjgs.144. 4.0531.

Floyd P.A., Shail R., Leveridge B.E., Franke W. Geochemistry and provenance of Rhenoher-cynian synorogenic sandstone: Implications fortectonic environment discrimination. In: Developments in Sedimentary Provenance (Morton A., Todd S.P., Haughton P.D.W. eds), Geological Society Special Publication 57, 1990, pp. 173-88, Geological Society of London, London.

Floyd P.A., Winchester J.A. and Park R.G. Geochemistry and tectonic setting of Lewisian clastic metasediments from the Early Proterozoic Loch Maree Group of Gairloch, N.W. Scotland. Precambrian Research, Vol.45, 1989, pp. 203-214, http://dx.doi.org/10.1016/0301-9268(89)90040-5.

Harnois L. The CIW index: A new chemical index of weathering. Sedimentary Geology, Vol. 55, No. 3-4, 1988, pp. 319-322, https://doi.org/10.1016/0037-0738(88)90137-6.

Hauhnar M., Lalnunmawia J., Dawngliana O.M.S. Geochemistry of Barail sandstone in Champhai, Mizoram: Implications on provenance and weathering history. J. Earth Syst. Sci., Vol. 130, No. 27, 2021, pp. 2-19, https://doi.org/10.1007/s12040-020-01515-9.

Herron M.M. Geochemical classification of terrigenous sands and shales from core or log data. Journal of Sedimentary Petrology, Vol. 58, No. 5, 1988, pp. 820-829.

Kangarli T.N. Mass overthrust within the structure of Greater Caucasus (Azerbaijan). In: The modern problems of geology and geophysics of Eastern Caucasus and the South Caspian Depression. 34th International Geological Congress. Special Issue Papers. Nafta-Press. Baku, 2012, pp. 163-201.

Kroonenberg S.B. Effects of provenance, sorting and weathering on the geochemistry of fluvial sands from different tectonic and climatic environments. In: Proc. 29th Int. Geol. Congr. Part A. (Kumon F., Yu K.M. eds.), Kyoto, Japan 1992, VSP Publ., Utrecht, 1994, pp. 69-81.

McLennan S.M. Rare earth elements in sedimentary rocks: influence of provenance and sedimentary processes. In: Geochemistry and Mineralogy of Rare Earth Elements (Lipin B.R. and McKay G.A., eds.), De Gruyter. Berlin, Vol. 21, No. 1, 1989, pp. 169-200, https://doi.org/10.1515/97815015 09032-010.

McLennan S.M. Weathering and global denudation. The Journal of Geology, Vol. 101(2), 1993, pp. 295-303. https://doi.org/ 10.1086/648222.

Md. Masidul Haque, Mrinal Kanti Roy. Sandstone-Shale Geochemistry of Miocene Surma Group in Bandarban Anticline, SE Bangladesh: Implications for Provenance, Weathering, and Tectonic Setting. Earth Sciences, Vol. 9(1), 2020, 38-51, https://doi.org/10.11648/j.earth.20200901.15.

Murali A.V., Parthasarathy R., Mahadevan T.M., Das M.S. Trace element characteristics, REE patterns and partition coefficients of zircons from different geological environments

Cox R., Lowe D.R., Cullers R.L. The influence of sediment recycling and basement composition on evolution of mudrock chemistry in the Southwestern United States. Geochimica et Cosmochimica Acta, Vol. 59, No. 14, 1995, pp. 2919-2940, https://doi.org/10.1016/0016-7037(95)00185-9.

Fedo C.M., Nesbitt H.W., Young G.M. Unravelling the effects of potassium metasomatism in sedimentary rocks and paleosols, with implications for palaeo-weathering conditions and provenance. Geology, Vol. 23, No. 10, 1995, pp. 921-924, https://doi.org/10.1130/0091-7613 (1995)023<0921: UTEOPM>2.3.CO;2.

Floyd P.A. and Leveridge B.E. Tectonic environment of the Devonian Gramscatho Basin South Cornwall: Framework mode and geochemical evidence from turbiditic sandstones. Journal of the Geological Society (London), Vol. 144, 1987, pp. 531-542, http://dx.doi.org/10.1144/gsjgs.144.4.0531.

Floyd P.A. and Leveridge B.E. Tectonic environment of the Devonian Gramscatho Basin South Cornwall: Framework Mode and Geochemical Evidence from Turbiditic Sandstones. Journal of the Geological Society (London), Vol. 144, 1987, pp. 531-542, http://dx.doi.org/10.1144/gsjgs.144.4.0531.

Floyd P.A., Shail R., Leveridge B.E., Franke W. Geochemistry and provenance of Rhenoher-cynian synorogenic sandstone: Implications fortectonic environment discrimination. In: Developments in Sedimentary Provenance (Morton A., Todd S.P., Haughton P.D.W. eds), Geological Society Special Publication 57, 1990, pp. 173-88, Geological Society of London, London.

Floyd P.A., Winchester J.A. and Park R.G. Geochemistry and tectonic setting of Lewisian clastic metasediments from the Early Proterozoic Loch Maree Group of Gairloch, N.W. Scotland. Precambrian Research, Vol.45, 1989, pp. 203-214, http://dx.doi.org/10.1016/0301-9268(89)90040-5.

Harnois L. The CIW index: A new chemical index of weathering. Sedimentary Geology, Vol. 55, No. 3-4, 1988, pp. 319-322, https://doi.org/10.1016/0037-0738(88)90137-6.

Hauhnar M., Lalnunmawia J., Dawngliana O.M.S. Geochemistry of Barail sandstone in Champhai, Mizoram: Implications on provenance and weathering history. J. Earth Syst. Sci., Vol. 130, No. 27, 2021, pp. 2-19, https://doi.org/10.1007/s12040-020-01515-9.

Herron M.M. Geochemical classification of terrigenous sands and shales from core or log data. Journal of Sedimentary Petrology, Vol. 58, No. 5, 1988, pp. 820-829.

Kangarli T.N. Mass overthrust within the structure of Greater Caucasus (Azerbaijan). In: The modern problems of geology and geophysics of Eastern Caucasus and the South Caspian Depression. 34th International Geological Congress. Special Issue Papers. Nafta-Press. Baku, 2012, pp. 163-201.

Kroonenberg S.B. Effects of provenance, sorting and weathering on the geochemistry of fluvial sands from different tectonic and climatic environments. In: Proc. 29th Int. Geol. Congr. Part A. (Kumon F., Yu K.M. eds.), Kyoto, Japan 1992, VSP Publ., Utrecht, 1994, pp. 69-81.

McLennan S.M. Rare earth elements in sedimentary rocks: influence of provenance and sedimentary processes. In: Geochemistry and Mineralogy of Rare Earth Elements (Lipin B.R. and McKay G.A., eds.), De Gruyter. Berlin, Vol. 21, No. 1, 1989, pp. 169-200, https://doi.org/10.1515/9781501509032-010.

McLennan S.M. Weathering and global denudation. The Journal of Geology, Vol. 101(2), 1993, pp. 295-303. https://doi.org/ 10.1086/648222.

Md. Masidul Haque, Mrinal Kanti Roy. Sandstone-Shale Geochemistry of Miocene Surma Group in Bandarban Anticline, SE Bangladesh: Implications for Provenance, Weathering, and Tectonic Setting. Earth Sciences, Vol. 9(1), 2020, 38-51, https://doi.org/10.11648/j.earth.20200901.15.

– A case study on Indian zircons. Geochimica et Cosmochimica Acta, Vol. 47, 1983, pp. 2047-2052.
Nesbitt H.W. and Young G.M. Early Proterozoic climates and plate motions inferred from major element chemistry of lutites. Nature, Vol. 299, 1982, pp. 715-717, https://doi.org/10.1038/299715a0.
Nesbitt H.W. and Young G.M. Prediction of some weathering trends of plutonic and volcanic rocks based on thermodynamic and kinetic considerations. Geochimica et Cosmochimica Acta, Vol. 48, No. 7, 1984, pp. 1523-1534, DOI:10.1016/0016-7037(84)90408-3.
Pettijohn F.J., Potter P.E., Siever R. Sand and sandstone. Springer-Verlag. New York, 1973, 618 p.
Rodrigo J.D., Gabo-Ratio J.A.S., Queaño K.L., Fernando A.G.S., Silva L.P., Yonezu K., Zhang Y. Geochemistry of the Late Cretaceous Pandan Formation in Cebu Island, Central Philippines: Sediment contributions from the Australian plate margin during the Mesozoic. The Depositional Record, Vol. 6(2), 2020, pp. 309-330, DOI:10.1002/dep2.103.
Roser B.P. and Korsch R.J. Determination of Tectonic Setting of Sandstone-Mudstone Suites Using SiO2 Content and K2O/Na2O Ratio. Journal of Geology, Vol. 94, 1986, pp. 635-650, https://doi.org/10.1086/629071.
Rustamov M.I. Geodynamics and magmatism of the Zagros-Caucasus Segment in the Phanerozoic. Palmarium Academic Publishing. 2016, 543 p. (in Russian).
Schieber J. A combined petrographical-geochemical provenance study of the Newland formation, Mid-Proterozoic of Montana. Geological Magazine, Vol. 129, 1992, pp. 223-237.
Taylor S.R. and McLennan S.M. The continental crust: Its composition and evolution. Blackwell Scientific Publications. Oxford, 1985, pp. 1-312.
Taylor S.R., McLennan S.M. The continental crust: Its composition and evolution. Oxford, London, Edinburgh, Boston, Palo Alto, Melbourne: Blackwell Scientific. Geological Magazine, Vol. 122(6), 1985, pp. 673-674, DOI:10.1017/S0016756800032167.
Murali A.V., Parthasarathy R., Mahadevan T.M., Das M.S. Trace element characteristics, REE patterns and partition coefficients of zircons from different geological environments – A case study on Indian zircons. Geochimica et Cosmochimica Acta, Vol. 47, 1983, pp. 2047-2052.
Nesbitt H.W. and Young G.M. Early Proterozoic climates and plate motions inferred from major element chemistry of lutites. Nature, Vol. 299, 1982, pp. 715-717, https://doi.org/10.1038/299715a0.
Nesbitt H.W. and Young G.M. Prediction of some weathering trends of plutonic and volcanic rocks based on thermodynamic and kinetic considerations. Geochimica et Cosmochimica Acta, Vol. 48, No. 7, 1984, pp. 1523-1534, DOI:10.1016/0016-7037(84)90408-3.
Pettijohn F.J., Potter P.E., Siever R. Sand and sandstone. Springer-Verlag. New York, 1973, 618 p.
Rodrigo J.D., Gabo-Ratio J.A.S., Queaño K.L., Fernando A.G.S., Silva L.P., Yonezu K., Zhang Y. Geochemistry of the Late Cretaceous Pandan Formation in Cebu Island, Central Philippines: Sediment contributions from the Australian plate margin during the Mesozoic. The Depositional Record, Vol. 6(2), 2020, pp. 309-330, DOI:10.1002/dep2.103.
Roser B.P. and Korsch R.J. Determination of Tectonic Setting of Sandstone-Mudstone Suites Using SiO2 Content and K2O/Na2O Ratio. Journal of Geology, Vol. 94, 1986, pp. 635-650, https://doi.org/10.1086/629071.
Schieber J. A combined petrographical-geochemical provenance study of the Newland formation, Mid-Proterozoic of Montana. Geological Magazine, Vol. 129, 1992, pp. 223-237.
Taylor S.R. and McLennan S.M. The continental crust: Its composition and evolution. Blackwell Scientific Publications. Oxford, 1985, pp. 1-312.
Taylor S.R., McLennan S.M. The continental crust: Its composition and evolution. Oxford, London, Edinburgh, Boston, Palo Alto, Melbourne: Blackwell Scientific. Geological Magazine, Vol. 122(6), 1985, pp. 673-674, DOI:10.1017/S0016756800032167.

ПЕТРОГРАФИЯ И ГЕОХИМИЯ НИЖНЕМЕЛОВЫХ ОТЛОЖЕНИЙ ВАНДАМСКОЙ ЗОНЫ (ЮЖНЫЙ СКЛОН БОЛЬШОГО КАВКАЗА): ПАЛЕОВЫВЕТРИВАНИЕ, ИСТОЧНИКИ СНОСА И ТЕКТОНИЧЕСКАЯ ОБСТАНОВКА

Гулиев Э.Х.
Министерство науки и образования Республики Азербайджан, Институт геологии и геофизики AZ1143, Баку, просп. Г.Джавида, 119: guliyevemin@outlook.com

Резюме. Исследование посвящено палеогеографическим условиям выветривания, источникам сноса и геодинамическим условиям формирования неокомских отложений. Основное внимание уделено кепучской и гырхбулагской свитам Вандамской тектонической зоны, расположенной на северном борту Южно-Кавказской микроплиты, которая характеризуется комплексом меловых флишевых и вулканогенными формаций. Посредством интеграции петрографических и геохимических данных исследование направлено на выявление характерных геохимических признаков, отражающих источники осадков, процессы выветривания и среды осадконакопления, что способствует углублению понимания геодинамической эволюции региона. Петрографический анализ песчаников показывает, что они состоят преимущественно из обломков пород, кварца и полевого шпата, акцессорных минералов и глинистого матрикса, превышающего 15%, что позволяет классифицировать их как литарениты, и подчеркивает преобладание обломков вулканических и метаморфических пород, а также аутигенного кальцитового цемента. Геохимические индикаторы палеовыветривания, такие как индекс химического выветривания (CIA), индекс выветривания (CIW) и индекс выветривания плагиоклаза (PIA), указывают на низкую и умеренную степень выветривания областей источника сноса. Геохимический анализ терригенных пород указывает на их смешанное происхождение, преимущественно из кислых и средних магматических пород, что соотносится с тектоническими условиями континентальной островной дуги. Дискриминационные диаграммы (SiO_2–K_2O/Na_2O, Al_2O_3/SiO_2 – Fe_2O_3+MgO, La–Th–Sc, Ti/Zr–La/Sc, Eu/Eu*–Gd_N/Yb_N) указывают на размещение образцов в полях активной континентальной окраины и континентальной островной дуги, указывая на субдукционное происхождение. Эти результаты подчёркивают влияние тектонических процессов на геохимические характеристики терригенных пород.

Ключевые слова*: источники сноса, геодинамический режим, палеовыветривание, Вандамская зона, кепучская и гырхбулагская свиты*

VƏNDAM TEKTONİK ZONASININ (BÖYÜK QAFQAZIN CƏNUB YAMACI) ALT TƏBAŞİR ÇÖKÜNTÜLƏRİNİN PETROQRAFİYASI VƏ GEOKİMYASI: PALEOAŞINMA, AŞINMA MƏNBƏLƏRİ VƏ TEKTONİK ŞƏRAİT

Quliyev E.X.
Azərbaycan Respublikası Elm və Təhsil Nazirliyi, Geologiya və Geofizika İnstitutu, Azərbaycan
AZ1073, Bakı, H. Cavid prospekti, 119: guliyevemin@outlook.com

Xülasə. Bu tədqiqat Alt Təbaşir yaşlı çöküntü laylarının paleocoğrafi aşınma şəraitini, gətirilmə mənbələrini və geodinamik şəraitini araşdırmağa həsr olunmuşdur. Tədqiqatda əsas diqqət Cənubi Qafqaz mikroplitəsinin şimal cinahında yerləşən və mürəkkəb Təbaşir yaşlı fliş və vulkanogen formasiyaları ilə xarakterizə olunan Vəndam tektonik zonasındakı Kepuç və Qırxbulaq lay dəstələrinə yönəldilmişdir. Petroqrafik və geokimyəvi məlumatların inteqrasiyası vasitəsilə bu tədqiqat çöküntü mənbələrini, aşınma proseslərini və çökmə mühitlərini əks etdirən xarakterik geokimyəvi göstəriciləri aşkar etməklə, regionun geodinamik inkişafını daha dərindən anlamağı hədəfləyir. Qumdaşlarının petroqrafik təhlili zamanı onların əsasən süxur fraqmentlərindən, kvarsdan və çöl şpatından ibarət olduğunu, 15%-dən artıq gil matriksinə malik olduğunu göstərir ki, bu da onları litarenitlər kimi təsnif etməyə imkan verir. Petroqrafik metodun tətbiqi nəticəsində süxurlarda vulkanik qırıntıların miqdarı metamorfik və çökmə mənşəli qırıntılardan daha çox olduğu, həmçinin sementin əsasən karbonat tərkibli və kalsitdən ibarət olduğu aydınlaşmışdır. Paleoaşınma üçün geokimyəvi göstəricilər, o cümlədən Kimyəvi Aşınma İndeksi (CIA), Aşınma İndeksi (CIW) və Plagioklazın Aşınma İndeksi (PIA), aşınma mənbələrinin zəif və orta dərəcədə aşındığını göstərir. Mənşə analizi göstərir ki, çöküntü materialları əsasən turş və orta maqmatik süxur növlərindən ibarət qarışıq mənşədən gəlir və bu kontinental ada qövsü tektonik mühiti ilə uyğundur. Diskriminasiya diaqramları (SiO_2-K_2O/Na_2O, Al_2O_3/SiO_2 – Fe_2O_3+MgO, La–Th–Sc, Ti/Zr–La/Sc, Eu/Eu*-Gd_N/Yb_N) nümunələrin aktiv kontinental kənar və kontinental ada qövsü sahələrində yerləşdiyini və subduksiya ilə əlaqəli çöküntü mənbəyinə işarə etdiyini göstərir. Bu analiz tektonik proseslərin terrigen süxurların geokimyəvi xüsusiyyətlərinin formalaşmasında mühüm rol oynadığını vurğulayır.

Açar sözlər: *aşınma mənbələri, geodinamik rejim, paleoaşınma, Vəndam zonası, Kepuç və Qırxbulaq lay dəstələri*